

Very high dielectric strength for dielectric elastomer actuators in liquid dielectric immersion

La, Thanh-Giang; Lau, Gih Keong

2013

La, T. G., & Lau, G. K. (2013). Very high dielectric strength for dielectric elastomer actuators in liquid dielectric immersion. *Applied physics letters*, 102(19).

<https://hdl.handle.net/10356/95759>

<https://doi.org/10.1063/1.4806976>

© 2013 IP Publishing LLC. This paper was published in *Applied Physics Letters* and is made available as an electronic reprint (preprint) with permission of IP Publishing LLC. The paper can be found at the following official DOI:[<http://dx.doi.org/10.1063/1.4806976>]. One print or electronic copy may be made for personal use only. Systematic or multiple reproduction, distribution to multiple locations via electronic or other means, duplication of any material in this paper for a fee or for commercial purposes, or modification of the content of the paper is prohibited and is subject to penalties under law.

Downloaded on 23 Aug 2022 05:02:47 SGT

Very high dielectric strength for dielectric elastomer actuators in liquid dielectric immersion

Thanh-Giang La and Gih-Keong Lau

Citation: *Appl. Phys. Lett.* **102**, 192905 (2013); doi: 10.1063/1.4806976

View online: <http://dx.doi.org/10.1063/1.4806976>

View Table of Contents: <http://apl.aip.org/resource/1/APPLAB/v102/i19>

Published by the [American Institute of Physics](#).

Additional information on *Appl. Phys. Lett.*

Journal Homepage: <http://apl.aip.org/>

Journal Information: http://apl.aip.org/about/about_the_journal

Top downloads: http://apl.aip.org/features/most_downloaded

Information for Authors: <http://apl.aip.org/authors>

ADVERTISEMENT

The advertisement banner features a dark orange background with a textured, golden-brown pattern. At the top, the 'AIP Applied Physics Letters' logo is displayed in white. Below the logo, there is a white envelope icon on the left. In the center, the text 'Accepting Submissions in Biophysics and Bio-Inspired Systems' is written in white. To the right of this text is a white button with the text 'Submit Today' in orange. On the far right, the 'AIP Publishing' logo is shown in white on a dark orange square background.

Very high dielectric strength for dielectric elastomer actuators in liquid dielectric immersion

Thanh-Giang La and Gih-Keong Lau

School of Mechanical and Aerospace Engineering, Nanyang Technological University, Singapore 639798

(Received 4 January 2013; accepted 27 April 2013; published online 14 May 2013)

This letter reported that a dielectric elastomer actuator (3M VHB), which is immersed in a liquid dielectric bath, is enhanced tremendously in dielectric strength up to 800 MV/m, as compared to 450 MV/m for the actuator operated in air. The bath consists of silicone oil (Dow Corning Fluid 200 50cSt), which is 6.5 times more thermally conductive than air, and it is found able to maintain the actuator at a stable temperature. As a result, the oil-immersed dielectric elastomer actuator is prevented from local thermal runaway, which causes loss of electrical insulation, and consequently avoids the damage by electromechanical instability. © 2013 AIP Publishing LLC.

[<http://dx.doi.org/10.1063/1.4806976>]

Dielectric elastomer actuators (DEAs) can produce large deformation under Maxwell stress, which is proportional to the square of the electric field.^{1–4} As a soft capacitor, DEA is liable to breakdown that limits the ultimate actuation strain. Dielectric elastomers without pre-stretch usually have a low dielectric strength, for example, 34 MV/m for the no-strained acrylic foam tape (VHB 4905).⁵ Pre-stretch was shown to help VHB dielectric elastomer increase substantially the dielectric strength to 300–400 MV/m.^{3,6–9} Such enhancement is attributed to air void suppression¹⁰ and dielectric stiffening¹¹ of the pre-stretched dielectric elastomer that avoids premature failure. Yet, the pre-stretched DEAs are still prone to failure by electromechanical or pull-in instability^{8,11–16} when activated by voltages.

According to Stark-Garton theory,¹⁷ softened polymer at elevated temperature may fail by mechanical collapse when stressed electrically. The theory predicts a critical dielectric strength of $E_c = \sqrt{Y/(\epsilon_r \epsilon_0)}$, in which Y is the Young's modulus and ϵ_r is the relative permittivity of the electrically stressed polymer slab, and ϵ_0 is the air permittivity. The value for critical strength is calculated to be 275 MV/m for VHB 4905 foam tape by using the properties: $Y=1.8$ MPa and $\epsilon_r = 2.68$, given by the 3M datasheet (see supplementary material¹⁸). If the pull-in instability can be avoided, DEA is believed to be able to sustain an even higher dielectric strength for producing higher actuation stress. DEA without electrodes¹⁹ was shown to avoid the electromechanical instability when activated by controlled charges. However, when usually activated by controlled voltages, the soft DEAs were not experimentally shown to survive the electro-mechanical instability.

Dielectric oil is typically impregnated in polypropylene film to prevent localized breakdown at the air gap of layer interfaces in power capacitors.²⁰ In a recent report by Yuan *et al.*,²¹ a thin layer of dielectric oil was coated on each single-walled-carbon-nanotube (SWCNT) electrodes in a 5 layered DEA stack in order to quench corona discharge and consequently extends the lifetime of DEAs. Quenching by dielectric oil is anticipated to enhance dielectric strength of DEAs. However, the oil quenched DEA was not reported to achieve a particularly high operating field at 250 MV/m.²¹ It

is thus not clear if dielectric oil quenching could help DEAs to operate beyond electromechanical instability.

In this letter, we shall show that dielectric liquid immersion helps prevent thermal runaway from breaking down DEA. As a result, the dielectric-liquid-immersed DEAs survived the electromechanical instability and achieved at a very high dielectric strength up to 800 MV/m, which is close to those for hard insulating plastic.²²

The immersion is in a bath of silicone oil (Dow Corning Fluid 200 50cSt), which has a boiling point of 65 °C, a thermal conductivity of 0.155 Wm⁻¹ K⁻¹, and a specific heat of 1473 Jkg⁻¹ K⁻¹ according to the datasheet (see supplementary material¹⁸). As silicone oil is 6.5 times more thermally conductive than air (with a thermal conductivity of 0.024 Wm⁻¹ K⁻¹), it can convect more heat than air following the law of heat transfer.²³ The immersion is expected to maintain the DEA temperature below the boiling temperature of the silicone oil. In addition, immersion in the silicone oil is expected to further help DEA to prevent partially discharge breakdown because the silicone oil is reported to have dielectric strength of 400 V/mil (Ref. 18) (or 15.7 MV/m) and a dielectric constant ranging from 2.72 to 2.75, which are greater than 3 MV/m dielectric strength at one atmospheric pressure and a unit dielectric constant of air, respectively.

In this work, samples of DEA were prepared from a 200% bi-axially pre-stretched VHB 4905 foam tape, which has a thickness of 55.0 μm as measured after pre-stretch. Borders of the pre-stretched dielectric film were supported on a square acrylic frame (60 mm × 60 mm). Graphite powders (TIMREX KS6) were applied by brushing on the pre-stretched dielectric film to form a pair of 15 mm diameter circular compliant electrodes, which has a surface resistivity measured to be 600 kΩ/□. During actuation test, DEA samples were completely immersed in the silicone oil bath as shown in Fig. 1. For comparison, samples of the same prepared DEAs were also tested in the usual condition, i.e., in air.

The DEA was activated using a high voltage supply (Spellman's CZE1000R). When the DEA is activated at an electric field \vec{E}' , its electrodes expand from an initial area A_0 to the activated area A' and the dielectric film reduces from an initial pre-stretched thickness t_{pre} to an activated thickness

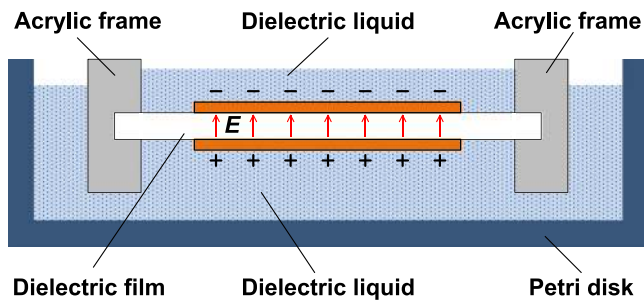


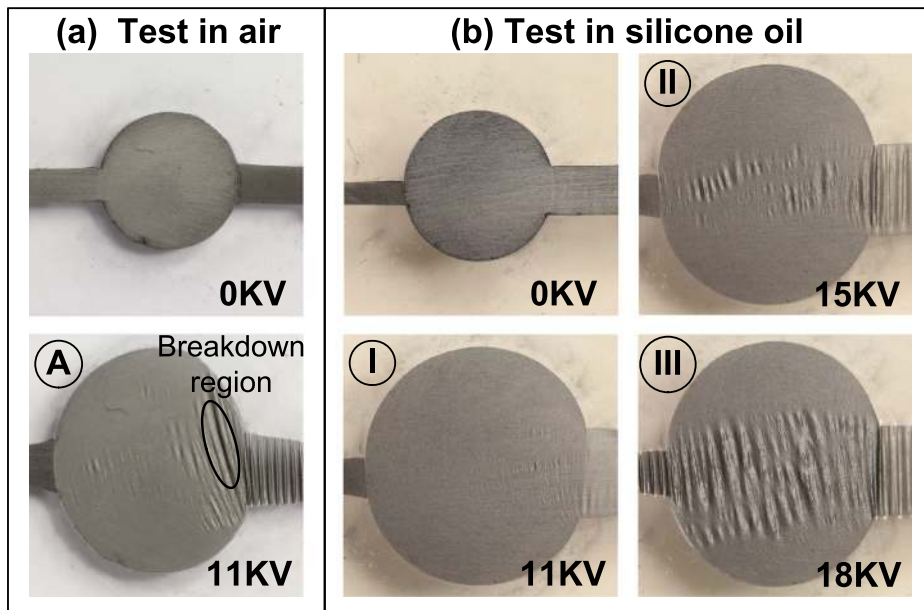
FIG. 1. A schematic (sectional view) showing the experimental setup, which has a DEA sample completely immersed in a silicone oil bath while the DEA is activated by high voltage.

t' . The areal strain is measured as $s_A = A'/A_0 - 1$, while the activated thickness is calculated as $t' = t_{pre}/(s_A + 1)$, on the assumption that the dielectric film that is incompressible. In turn, the true electric field is calculated as $\tilde{E}' = V/t'$, according to Ref. 7. As the voltage was ramped up during DEA activation, leakage current was monitored continuously using a digital multimeter (Agilent 34410A) and a NI data logger while photographs for the activated DEA were captured using a digital camera.

Electromechanical or pull-in instability of DEAs is often accompanied by thinning down in thickness and severe

wrinkles^{8,9,14,24,25} that indicate the loss of tension in the pre-stretched dielectric film. Such pull-in instability was also observed in our test of DEA samples. The DEA sample, which was tested in air, nearly failed at 11 kV and it exhibited a distorted electrode shape and irregular-pitch wrinkles near the defective spot as shown in Fig. 2(a) (image A). On the other hand, the DEA sample, which was tested in the liquid dielectric bath, did not fail at 11 kV while mild wrinkles appeared on the dielectric film (see image I in Fig. 2(b)). Interestingly, as driving voltage went beyond 11 kV, the oil-immersed DEA continued to work even though the wrinkles turned from mild (see image II at 15 kV) to severe (see the image III at 18 kV).

Figure 2(b) showed actuation of the DEAs as a function of the applied electric field. A similar trend of actuation was observed for both samples tested in either air or oil immersion. The areal actuation strains increase at a decreasing rate with respect to the applied electric field. The areal actuation strains are almost independent of the increasing electric field above 400 MV/m because the active dielectric film, which was pre-stretched, lost tension and buckled into wrinkles that were accompanied primarily by thickness reduction but little areal expansion. Similar observation on how wrinkles affect the areal actuation of dielectric elastomer was previously



(c) Area strain vs. Electric field

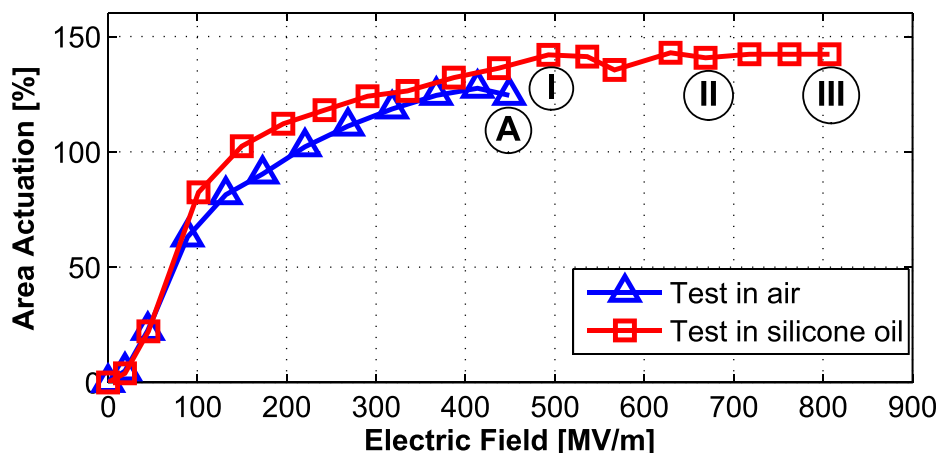
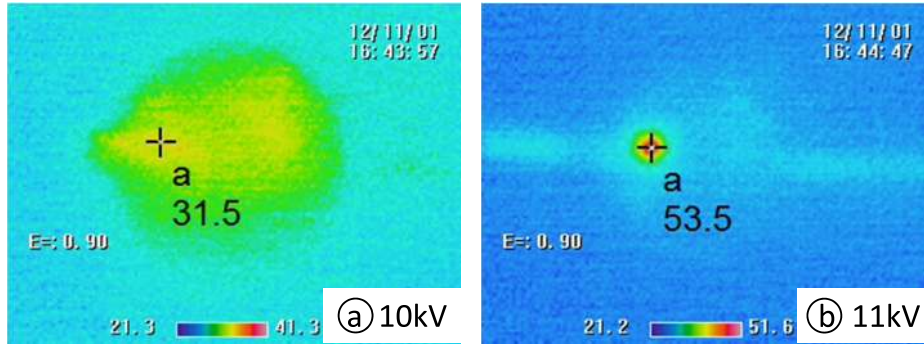


FIG. 2. Electromechanical activation of DEAs in either the air or the oil immersion: (a) Photographs showing electrode expansion for a DEA when tested in air. Wrinkles and sparks at spot were observed on dielectric film when the DEA breaks down at 11 kV (or 450 MV/m). (b) Photographs showing electrode expansion for a DEA when tested in the silicone oil immersion. Wrinkles appear changing from mild to severely undulated and sagging as the driving voltage increases from 11 kV to 18 kV, but the oil immersed DEA did not break down. (c) A graph showing areal strain of the activated DEAs as a function of electric field until breakdown.

(a) Test in air



(a) Test in silicone oil

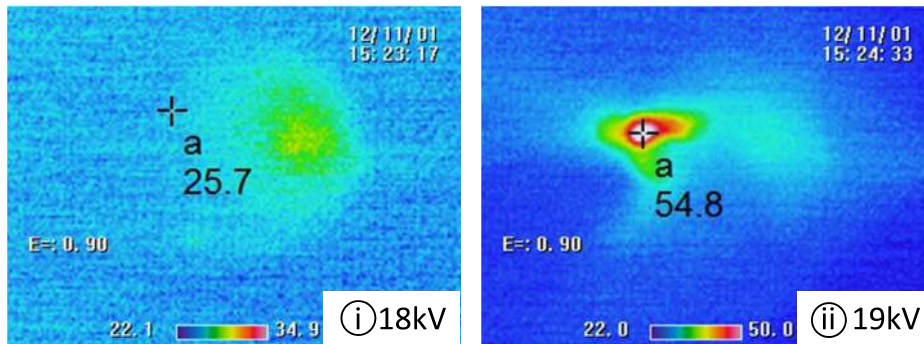


FIG. 3. Thermography of the activated DEAs: (a) two thermograms of a DEA sample in air at 10kV and 11kV, respectively. The right thermogram showed that a hot spot occurred at the puncture when the DEA in air breaks down at 11kV. (b) two thermograms of silicone oil bath, which immerses a DEA sample that is activated at 18kV and 19kV, respectively. Right thermogram showed that a distorted hot spot happens on the oil surface and it indicates oil circulation and Joule heating at the puncture of DEA, which breaks down at 19kV.

reported by Pelrine *et al.*³ Despite the similar actuation trend, the oil-immersed DEA can sustain a much higher voltage 18kV as compared to 11kV of the DEA operated in air. The oil immersed DEA achieved a dielectric strength of 800 MV/m, as calculated from the 142% areal strain at 18kV. On the other hand, the DEA operated in air achieved a dielectric strength of 450 MV/m, as calculated from the 125% areal strain at 11kV. In short, the immersion in silicone oil enhanced the dielectric strength of DEA by 70% more than that in air.

When a dielectric film breaks down, corona discharges (sparks) are observed to happen at local spots over the wrinkled regions. The spots are believed to collapse under excessive Maxwell stress, which is induced by increased electric field.^{8,26,27} At the same time, leakage current may accelerate the collapse because it resistively heats up and softens the spots.²⁶ To monitor the temperature at the defective spots, thermograms of the DEA were captured using an infrared camera (NEC Thermo Shot F30W) with a pixel size of 156 μm × 156 μm).

When broken down in air at 11kV, the DEA sample is punctured at a defective spot, which coincides with the hot spot in the thermogram in Fig 3. The defective spot underwent a drastic temperature rise from 31.6°C to 53.5°C, as shown in Fig. 4(a), as the driving voltage was increased towards 11kV, at which terminal failure happened. The transient corona discharge at the puncture is expected to be higher in temperature, but not captured by the thermogram. Joule heating at the puncture is indicated in Fig. 4(b) by a current surge that remains high at 120 μA, which is the current limit of the high voltage supply.

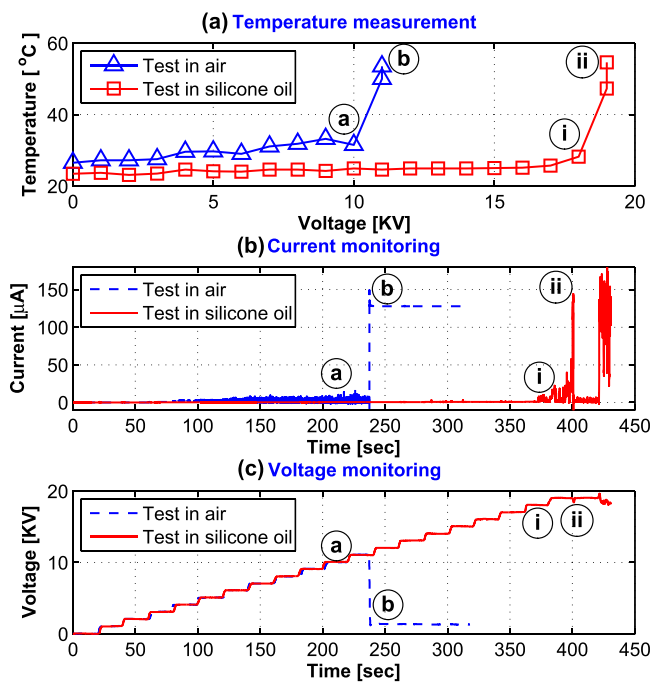


FIG. 4. Monitor of temperature and leakage current for DEA samples, which were activated by increasing voltages in air or oil immersion, respectively. (a) A graph showing temperature as a function of driving voltage at the punctured region of DEA sample. (b) Time histories of leakage current as the driving voltage is ramped up across the DEA. Leakage current surges when DEA breaks down. (c) Time histories of the driving voltage, which was increased incrementally until the breakdown of DEA. The voltage dips to low beyond the control when DEA breaks down in air at 11kV.

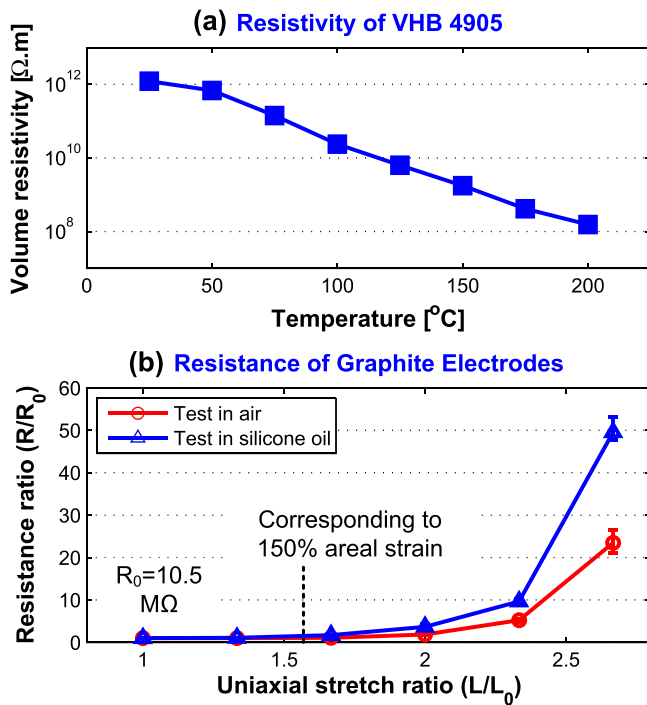


FIG. 5. (a) Temperature dependence of volume (or bulk) resistivity of a 200% biaxially pre-stretched VHB 4905 film (with a $55\ \mu\text{m}$ pre-stretched thickness). (b) Surface resistance of graphite powder electrodes as a function of uniaxial stretch ratio.

When tested in the silicone oil bath up to 18 kV, the DEA sample is maintained a rather stable temperature and minimal leakage current. As a result of oil immersion, terminal failure of the DEA is deferred from 11 kV to 19 kV. The oil-immersed DEA survived the first thermal runaway at 19 kV, which was quenched by oil. But, it did not survive the second thermal runaway, which caused tear and rupture of the pre-stretched dielectric film. During the first thermal runaway at 19 kV, a hot spot of $54.8\ ^{\circ}\text{C}$ was observed from the thermogram (see Fig. 3(b) image (ii)) and it was accompanied by current surge as shown in Fig. 4.

These experimental results showed that the oil-immersed DEA survived the nearly pull-in state which is indicated with severe wrinkles, but the DEA tested in air did not. This suggests that the silicone oil bath has successfully quenched thermal runaway that could have damaged the DEA. Hence, “thermal runaway” or thermal breakdown is believed to be the culprit to cause DEA a terminal failure. This hypothesis is further supported by the fact that dielectric

resistivity reduces substantially with temperature rise according to Refs. 26 and 28 and our recent measurement of VHB bulk resistivity.

In this work, we measured the bulk resistivity from a VHB sample, which consists of a 200% bi-axially pre-stretched VHB film and is configured into a capacitor by cladding the VHB film with a pair of copper foil electrodes (with an electrode area of $A = 15\ \text{mm} \times 15\ \text{mm}$). During measurement, the elastomeric sample was subjected to an elevated temperature T in a furnace and its leakage current $I(T)$ under a constant voltage $V_{dc} = 100\ \text{V}$ was measured using a picometer (Keithley 6485). The bulk resistivity is calculated as: $\rho = V_{dc}/I(T) \times A/t$, in which A is the cross section area of the capacitor and t is its thickness.

Fig. 5(a) showed that bulk resistivity of pre-stretched VHB4905 is strongly dependent on temperature. The measured bulk resistivity decreases exponentially from $1.2 \times 10^{12}\ \Omega\text{m}$ to $1.5 \times 10^8\ \Omega\text{m}$, which amounts to a 4-order drop, when the VHB temperature rises from $25\ ^{\circ}\text{C}$ to $200\ ^{\circ}\text{C}$. Hence, this leads us to believe that thermal runaway happens because resistivity reduces with temperature rise at the pull-in hot spot, in addition to the effect from electric field.²⁷

In addition, the silicone oil bath is expected to have some effect on electrode resistance. Fig. 5(b) showed graphite electrode resistance as a function of uni-axial stretch. The presence of oil did not change the initial resistance (10.5 M Ω) of the un-stretched electrode, but it affected the apparent resistance of the stretched electrode. For example, the oil-immersed electrode, which was uniaxially stretched 1.58 time (corresponding to 150% areal strain), exhibited 20% more resistance than that in air. This resistance increment in the presence of oil is attributed to oil seepage between the dislocated graphite particles. However, the effect of silicone oil on the stretched electrode resistance is not as dominant as its effect on the dielectric temperature, which in turn greatly influences the bulk resistivity and electrical breakdown of the dielectric elastomer.

Table I lists the reported dielectric strengths for VHB acrylic elastomers. The reported strengths vary substantially because of the different conditions of pre-stretch, dielectric film thickness, and compliant electrode materials. A high dielectric strength as much as 412 MV/m was reported for a bi-axially prestretched (4×4) VHB DEA with conductive grease electrodes. Recently, a 500 MV/m strength was also demonstrated for a pre-stretched VHB film, which was clamped between two stiff plastic layers.⁹ However, the

TABLE I. Breakdown strength of VHB films or DEAs.

Work	Compliant electrode	Dielectric elastomer	Pre-stretch ratio (x,y)	Breakdown strength (MV/m)	Area strain (%)
Shankar <i>et al.</i> ⁵	Ag grease	VHB 4910	(0,0)	34	12.4
Pelrine <i>et al.</i> ³	Carbon grease	VHB 4910	(6.4,1.75)	239	215
Pelrine <i>et al.</i> ³	Carbon grease	VHB 4910	(4,4)	412	158
Kofod <i>et al.</i> ⁷	Brass plate	VHB 4910	(6,6)	218	0
Huang <i>et al.</i> ⁹	Copper wires	VHB 4905	(6,6)	500	0
Yuan <i>et al.</i> ²⁹	SWCNTs	VHB 4905	(4,4)	340	140–160
Low <i>et al.</i> ³⁰	Electro-less silver	VHB 9473PC	(2.5,2.5)	350	50
Current work	Graphite powder	VHB 4905	(3,3)	>800	142

clamped VHB film cannot actuate. In comparison, a very high dielectric strength 800 MV/m is demonstrated by our silicone-oil-immersed VHB DEA.

With such high dielectric strength, the oil-immersed DEAs can not only operate reliably at high electric fields but also offer the benefit of higher force generation. According to the electrostatics formula, the induced Maxwell stress at the 800 MV/m is calculated to be as much as 12.7–13.3 MPa, based on the reported dielectric constant 4.5–4.7 for the pre-stained VHB 4905/4910 tape.⁷ In future, such oil-immersed DEAs can be configured to work against an even higher pre-load or external load, for example, in a cylindrical shape for lifting a heavy deadweight.

In conclusion, this work showed that silicone oil immersion can prevent thermal runaway, which causes loss of electrical insulation at defective spots, from damaging dielectric elastomer actuators. As a result, the oil-immersed DEAs demonstrated a large actuation at a very high dielectric strength 800 MV/m, even in the presence of severe wrinkles that indicate imminence of pull-in instability. This work showed that the oil-immersed DEAs have potential to sustain a very high Maxwell stress.

This work was with partial financial support by the Nanyang Technological University (NTU) of Singapore through the Start-Up Grant and Defense Science and Technology Agency (DSTA) of Singapore through Defence Innovation Research Program (DIRP).

- ¹R. E. Pelrine, R. D. Kornbluh, and J. P. Joseph, *Sens. Actuators, A* **64**, 77–85 (1998).
- ²R. Kornbluh, R. Pelrine, J. Joseph, R. Heydt, Q. B. Pei, and S. Chiba, *Proc. SPIE* **3669**, 149–161 (1999).
- ³R. E. Pelrine, R. D. Kornbluh, Q. B. Pei, and J. Joseph, *Science* **287**, 836–839 (2000).
- ⁴R. Pelrine, R. Kornbluh, J. Joseph, R. Heydt, Q. Pei, and S. Chiba, *Mater. Sci. Eng., C* **11**, 89–100 (2000).
- ⁵R. Shankar, T. K. Ghosh, and R. J. Spontak, *Macromol. Rapid Commun.* **28**, 1142–1147 (2007).
- ⁶G. Kofod, R. Kornbluh, R. Pelrine, and P. Sommer-Larsen, *Proc. SPIE* **4329**, 141–147 (2001).
- ⁷G. Kofod, P. Sommer-Larsen, R. Kornbluh, and R. Pelrine, *J. Intell. Mater. Syst. Struct.* **14**, 787–793 (2003).
- ⁸J.-S. Plante and S. Dubowsky, *Int. J. Solids Struct.* **43**, 7727–7751 (2006).
- ⁹J. S. Huang, S. Shian, R. M. Diebold, Z. G. Suo, and D. R. Clarke, *Appl. Phys. Lett.* **101**, 122905 (2012).
- ¹⁰D. P. Muffoletto, K. M. Burke, and J. L. Zirnheld, *Proc. SPIE* **8340**, 834021 (2012).
- ¹¹X. Zhao and Z. Suo, *Phys. Rev. Lett.* **104**, 178302 (2010).
- ¹²X. Zhao and Z. Suo, *Appl. Phys. Lett.* **91**, 061921 (2007).
- ¹³X. Zhao and Z. Suo, *J. Appl. Phys.* **104**, 123530 (2008).
- ¹⁴C. Keplinger, M. Kaltenbrunner, N. Arnold, and S. Bauer, *Appl. Phys. Lett.* **92**, 192903 (2008).
- ¹⁵S. Koh, T. Li, J. Zhou, X. Zhao, W. Hong, J. Zhu, and Z. Suo, *J. Polym. Sci., Part B: Polym. Phys.* **49**, 504–515 (2011).
- ¹⁶P. Brochu and Q. Pei, *Macromol. Rapid Commun.* **31**, 10–36 (2010).
- ¹⁷K. Stark and C. Garton, *Nature* **176**, 1225–1226 (1955).
- ¹⁸See supplementary material at <http://dx.doi.org/10.1063/1.4806976> for given material properties of 3M VHB Adhesive Transfer Tapes and Dow Corning 200 Fluid 50cs (now known as Xiameter PMX-200 Silicone Fluid 50cs).
- ¹⁹C. Keplinger, M. Kaltenbrunner, N. Arnold, and S. Bauer, *Proc. Natl. Acad. Sci. U.S.A.* **107**, 4505–4510 (2010).
- ²⁰A. Tomago, T. Shimizu, Y. Iijima, and I. Yamauchi, *IEEE Trans. Electr. Insul.* **EI-12**, 293–301 (1977).
- ²¹W. Yuan, P. Brochu, S. Ha, and Q. Pei, *Sens. Actuators, A* **155**, 278–284 (2009).
- ²²X. Zhou, X. Zhao, Z. Suo, C. Zou, J. Runt, S. Liu, S. Zhang, and Q. Zhang, *Appl. Phys. Lett.* **94**, 162901 (2009).
- ²³F. P. Incropera and D. P. DeWitt, *Fundamentals of Heat and Mass Transfer*, 4th ed. (Wiley, New York, 2000), p. 493.
- ²⁴X. Zhao and Z. Suo, *Appl. Phys. Lett.* **95**, 031904 (2009).
- ²⁵J. Zhu, M. Kollosche, T. Lu, G. Kofod, and Z. Suo, *Soft Matter* **8**(34), 8840–8846 (2012).
- ²⁶L. Dissado and J. Fothergill, “Overview of electrical degradation and breakdown,” in *Electrical Degradation and Breakdown in Polymers* (Peter Peregrinus Ltd, 1992), pp. 62–66.
- ²⁷L. Di Lillo, A. Schmidt, D. A. Carnelli, P. Ermanni, G. Kovacs, E. Mazza, and A. Bergamini, *J. Appl. Phys.* **111**, 024904 (2012).
- ²⁸T. Gisby, S. Xie, E. Calius, and I. Anderson, *Proc. SPIE* **7642**, 764213 (2010).
- ²⁹W. Yuan, L. B. Hu, Z. B. Yu, T. Lam, J. Biggs, S. M. Ha, D. J. Xi, B. Chen, M. K. Senesky, G. Grner, and Q. Pei, *Adv. Mater.* **20**, 621–625 (2008).
- ³⁰S. H. Low, L. L. Shiau, and G. K. Lau, *Appl. Phys. Lett.* **100**, 182901 (2012).